International Journal of Minerals, Metallurgy and Materials
Volume 28, Number 2, February 2021, Page 231
https://doi.org/10.1007/s12613-020-2034-z

Selective reduction of carbon dioxide into amorphous carbon over activated natural magnetite

Zhong-qing Liu, Jian Zheng, Yi Wang, and Xu Liu

School of Chemical Engineering, Sichuan University, Chengdu 610065, China
(Received: 15 October 2019; revised: 3 March 2020; accepted: 4 March 2020)

Abstract: Natural magnetite formed by the isomorphism substitutions of transition metals, including Fe, Ti, Co, etc., was activated by mechanical grinding followed by H_2 reduction. The temperature-programmed reduction of hydrogen (H_2-TPR) and temperature-programmed surface reaction of carbon dioxide (CO_2-TPSR) were carried out to investigate the processes of oxygen loss and CO_2 reduction. The samples were characterized by X-ray diffraction (XRD), field emission scanning electron microscopy (FE-SEM), and energy-dispersive X-ray spectroscopy (EDS). The results showed that the stability of spinel phases and oxygen-deficient degree significantly increased after natural magnetite was mechanically milled and reduced in H_2 atmosphere. Meanwhile, the activity and selectivity of CO_2 reduction into carbon were enhanced. The deposited carbon on the activated natural magnetite was confirmed as amorphous. The amount of carbon after CO_2 reduction at 300°C for 90 min over the activated natural magnetite was 2.87wt% higher than that over the natural magnetite.

Keywords: carbon dioxide reduction; natural magnetite; isomorphism substitutions; grind activation; oxygen-deficient degree; amorphous carbon

1. Introduction

To some extent, CO_2 emission reduction can efficiently alleviate the global temperature rise and enable the use of non-renewable fuels [1]. The approaches for reducing CO_2 emission mainly include reduction and capture. Moreover, CO_2 can be reduced to various chemical high-added-value fuels via electrocatalysis, photocatalysis, and thermal catalysis [2]. For the electrocatalytic or photocatalytic method, the reaction can only be carried out under a certain overpotential because CO_2 molecule is extremely stable. The products are generally a mixture of gas and liquid containing 1–4 carbons due to the product selectivity, leading to difficulty in separation and transport [3−4]. While CO_2 capture requires a medium (certain beneficial geographical conditions), it cannot be widely adopted, and government support is needed [2]. Therefore, studying CO_2 reduction by thermal catalysis with cheap raw materials is necessary.

Since the last decades, natural magnetite has attracted much attention because of its extensive use. It can be used for drug delivery [5], degradation of organic pollutants [6], decomposition of H_2O_2 [7], and decomposition of CO_2 [8−12]. In the early 1990s, Tamaura and Tahata [13] reported that CO_2 could be completely decomposed to carbon over the oxygen-deficient magnetite $Fe_3O_{4-\delta}$ ($0 < \delta < 1$) at a low temperature near 300°C. This opened up a new study area of CO_2 decomposition as an expected route to address the "greenhouse effect" resulting from CO_2 emission. In a subsequent work, cation-deficient magnetite ($Fe_{3-\delta}O_4$, $0.2 > \delta > 0$) synthesized by the air oxidation of $Fe(OH)_2$ suspensions followed by H_2 reduction, oxygen-deficient magnetite, and wustite ($Fe_{1-x}O$) prepared by high-temperature thermal decomposition of iron oxalate (FeC_2O_4) were used for the reaction of CO_2 decomposition [14−15]. The study result showed that CO_2 could be decomposed to C by nearly 100% over these activated iron oxides at certain conditions. Álvarez-Torrellas *et al.* [16] enhanced the catalytic activity of natural magnetite by thermal treatments. In 2007, CO_2 was decomposed by mechanically milled wustite or ultrafine magnetite powders, and the decomposition products were confirmed to be graphite, amorphous carbon, and cementite (Fe_3C) [17−18], in which granularity and phase composition were regulated by tailoring the time and atmosphere of the high-power milling process. Compared with simple iron oxides such as magnetite or wustite, multi-metallic ferrites formed by isomorphism replacements are expected to produce more

Corresponding author: Zhong-qing Liu E-mail: lzq_301@126.com, liuzq_hgxy@scu.edu.cn

crystal defects and therefore provide more activated sites on their surfaces. Enhancing the ability and recycling stability of these iron oxides for CO_2 decomposition is advantageous. Thus, multi-metallic ferrites with oxygen deficiency have attracted increasing attention. They are represented by the general formula $M_xFe_{3-x}O_{4-\delta}$ and can be fabricated via H_2 reduction for $M_xFe_{3-x}O_4$ compounds, where M is a transition metal, such as Cu, Co, Ni, Mn, Cr, and Zn, and δ is the reduction degree. For instance, in previous studies, a series of ferrites MFe_2O_4 (M = Mn, Zn, Co, Ni, Cr) was prepared and used in the decomposition of CO_2 to C. The result demonstrated that $Ni_{0.49}Cu_{0.24}Zn_{0.24}Fe_2O_4$ possessed a higher activity and stability compared with binary compounds $(Ni,Cu,Zn)Fe_2O_4$ [8−12]. In addition, Kim *et al.* [19−20] prepared ultrafine $(Ni,Zn)Fe_2O_4$ powders using co-precipitation and hydrothermal methods and found that the activity of the powder prepared by the hydrothermal method was higher than that prepared by co-precipitation, which agrees with the results reported by other researchers [21–26]. The aforementioned results show that the activity and recycling stability can be significantly improved by mono- or multi-element doping of the ferrite. Among the dopants, Zn^{2+}, Ni^{2+}, and Cr^{3+} are preferred candidates. Certainly, these oxygen-deficient ferrites can be synthesized using different chemical routes. Only considering our country the substantive emissions of CO_2 are more than 2×10^{10} t before in 2000 [27–28], conventional preparation methods cannot meet the tremendous demands of the catalysts used for CO_2 decomposition, and they also bring new pollutants originated from their preparation processes.

Natural magnetite possesses a counter spinel structure, in which half of Fe^{3+} and all Fe^{2+} are located at the octahedral lattices, with the other half of Fe^{3+} at the tetrahedral positions. They are formed by the isomorphism substitutions of Al^{3+}, Ti^{4+}, Cr^{3+}, and V^{3+} for Fe^{3+} and also the substitutions of Mg^{2+}, Mn^{2+}, Zn^{2+}, Ni^{2+}, Co^{2+}, and Cu^{2+} for Fe^{2+}. Natural magnetite is greatly expected to serve as a catalyst for CO_2 decomposition considering its special structure that is similar to the ferrites synthesized artificially via a series of complicated chemical processes. However, CO_2 decomposition over natural magnetite has not been sufficiently researched so far. Hence, in this study, natural magnetite was mechanically milled and reduced in H_2 atmosphere for CO_2 decomposition. The study aims at presenting a facile and "green" approach to fabricate multi-metallic ferrites for the reduction of CO_2 into carbon with high selectivity.

2. Experimental

2.1. Materials and process route

Natural magnetite concentrates served as the raw material, with the main chemical compositions (wt%) of Fe 51.56, TiO_2 12.73, V_2O_5 0.564, Co 0.02, Ni 0.013, S 0.53, P 0.004, SiO_2 4.69, Al_2O_3 4.69, CaO 1.57, and MgO 3.91. Prior to mechanical milling, the concentrates were dried at 120°C for 12 h. The mechanical milling was performed under air with a ball-to-sample mass ratio of 15:1 and a rotation speed of 580 r/min for 6 h. Afterward, the sample was reduced in H_2 with a flux of 30 mL/min at 450°C for 90 min. Subsequently, the sample was cooled to 300°C using N_2. Then CO_2 reduction reaction on this sample was carried out at 300°C for 90 min (*in situ*), with a CO_2 flux of 30 mL/min. The mass of the sample treated by H_2 or CO_2 was 100 mg. As the control experiment, natural magnetite without mechanical milling was subjected to H_2 reduction and CO_2 reduction under the same conditions.

2.2. Characterization techniques

The morphologies of the samples were observed using field emission scanning electron microscopy (FE-SEM; Inspect F, FEI Corporation, Japan). The chemical composition was analyzed by energy-dispersive X-ray spectroscopy (Inca 350, Oxford Corporation, UK) coupled with scanning electron microscopy. The crystal structure was characterized using a Philips X'Pert PRO diffractometer (Netherlands) with Cu K_α radiation, employing a step size of 0.03°. The accelerating voltage was set at 40 kV with 40 mA flux. The software JADE 5.0 was used to index diffraction peaks. The Raman spectra were recorded with Lab Raman HR-800 (France), excited using 514.532 nm radiation argon ion laser with a power of 3.9 mW. The infrared radiation (IR, America) spectra were taken on a NEXUS470 spectrophotometer, using KBr disc and working in the absorption mode. The experimental conditions in the temperature-programmed reduction of hydrogen (H_2-TPR) process were as follows: 100 mg sample was embedded in a quartz tube with ϕ6 mm; the reducing atmosphere was pure H_2, the flow rate was 50 mL/min, and the heating rate was 10°C/min. The temperature-programmed surface reaction of carbon dioxide (CO_2-TPSR) experiments were conducted using the same apparatus as the TPR. The sample (100 mg) was heated from the ambient temperature to 850°C with a ramp-up of 10°C/min and CO_2 flow rate of 25 mL/min after the natural magnetite (hereafter denoted as NM) and the mechanically milled natural magnetite (hereafter denoted as MNM) were reduced in H_2 at 450°C for 90 min with a flow rate of 30 mL/min.

3. Results and discussion

3.1. H_2-TPR

The H_2-TPR spectra of the natural magnetite without and with mechanical milling are shown in Fig. 1. For this magnetite without mechanical milling, there are two reduction peaks, which are located at 466°C and 813°C, respectively. The peak at 466°C is very weak and corresponds to the reduction of iron oxides from a higher valence to a lower one, while the peak at 813°C is very strong and is ascribed to the

formation of metallic iron. Correspondingly, for the mechanically milled natural magnetite, the peaks shift to lower temperatures. One obvious peak at 450°C is observed, with the other peak at 751°C. The initial reduction peak attributed to oxygen loss is at 373°C for the MNM but at 591°C for the NM. There is a markedly negative shift of 218°C, as compared with the NM. Accordingly, to enhance the oxygen-deficient degree as much as possible, while keeping its spinel structure from destruction, the temperature of H_2 reduction should be selected as 450°C.

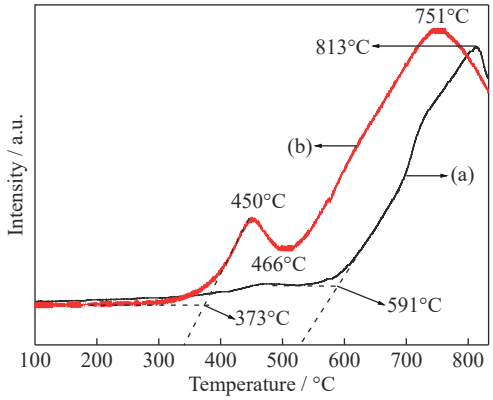

Fig. 1. H_2-TPR profiles of (a) NM and (b) MNM.

3.2. CO_2-TPSR

Fig. 2 shows the CO_2-TPSR spectra of the NM and the MNM. The samples were reduced in H_2 atmosphere at 450°C for 90 min and then cooled to the ambient temperature before CO_2-TPSR measurements. The intensities of CO_2 and CO are presented as black and red lines, respectively. It is clear that from 150 to 750°C, the CO_2 intensity for the MNM was significantly lower than that for the NM, the gap between the two samples was the largest at about 300°C and then slightly decreased with increasing temperature, suggesting that the MNM possesses a higher activity of CO_2 reduction. At 400°C, the CO signals for both specimens were observed. When the temperature was further increased to 450°C, the signal became more obvious. As a rule, CO_2 decomposition into carbon on the oxygen-deficient magnetite ($Fe_3O_{4-\delta}$, $0 < \delta < 1$) goes through an intermediate process that produces CO [22,29–31]. The reaction course can be depicted as follows:

$$CO_2 + 2e \rightarrow CO + O^{2-} \quad (1)$$

$$CO + 2e \rightarrow C + O^{2-} \quad (2)$$

Moreover, the lower the reduction degree δ, the greater the amounts of CO [32–33]. As shown in Fig. 2, for the two samples, the CO signal was much lower than the CO_2 signal from 150 to 500°C. Furthermore, from 150 to 687°C, the CO intensity of the MNM was always weaker than that of the NM. By contrary, when using $(Ni_xCu_{1-x})Fe_2O_4$ or M ferrites

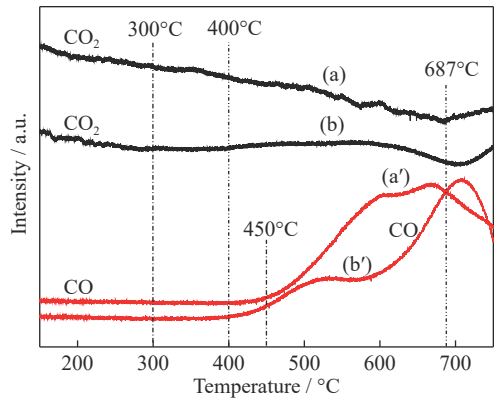

Fig. 2. CO_2-TPSR profiles of the samples reduced at 450°C: (a, a′) NM; (b, b′) MNM. The black lines are the intensity of CO_2, and the red lines correspond to the intensity of CO.

(M = Ni and Cu) as the catalyst for CO_2 decomposition, the marked CO intensity, which is close to CO_2, is detected within a wider temperature region, and the lower the temperature the stronger the CO signal [30,34]. Accordingly, it can be inferred that for the mechanically milled and freshly reduced natural magnetite, their higher selectivities of CO_2 reduction should be ascribed to their higher oxygen-deficient degrees and isomorphism substitutions of Fe, Ti, V, Co, Ni, and Al.

3.3. Transformation of phase composition

The X-ray diffraction (XRD) patterns of the NM and the MNM at various stages are illustrated in Figs. 3 and 4. For the NM, diffraction peaks from Fe_3O_4, $FeTiO_3$, $Mg_{1.55}Fe_{1.6}O_4$, and $MgFe_2O_4$ are observed, of which Fe_3O_4 and $FeTiO_3$ are the main crystalline phases, and only one compound of AB_2O_4 type (i.e., $MgFe_2O_4$) exists besides Fe_3O_4. After H_2 reduction, the diffraction peak of $Mg_{1.55}Fe_{1.6}O_4$ (JCPDS-80-0073) disappears while $(Co_{0.2}Fe_{0.8})Co_{1.2}Fe_{1.2}O_4$ (JCPDS-77-0426) phase appears. This increases the number of spinel phases, which is beneficial to CO_2 decomposition. After CO_2 decomposition, all diffraction peaks, which appeared in the former stages, become very weak, with disappearances of $MgFe_2O_4$ and $(Co_{0.2}Fe_{0.8})Co_{0.8}Fe_{1.2}O_4$ of spinel structure. Surprisingly, a new phase [Fe,Ni] exhibits the strongest signal as shown in curve (c) in Fig. 3. This suggests that for the NM, the spinel structure is destroyed greatly after CO_2 reduction reaction. As for the MNM, the phase evolvements at corresponding stages are distinctly different. Apart from Fe_3O_4, $MgFe_2O_4$ and $(Co_{0.2}Fe_{0.8})Co_{0.8}Fe_{1.2}O_4$ with AB_2O_4 spinel structures occur just after H_2 reduction. Note that the metallic phases of [Fe,Ni] and Fe were detected, while for the NM, the metal phases were observed only after CO_2 decomposition. Also, the stability of the crystalline structure, especially for the spinel phases Fe_3O_4, $(Co_{0.2}Fe_{0.8})Co_{0.8}Fe_{1.2}O_4$, and $MgFe_2O_4$, was evidently enhanced, while the diffraction peak of Fe_3O_4 phase for the NM has become very weak and markedly widened, with the latter two phases disappearing

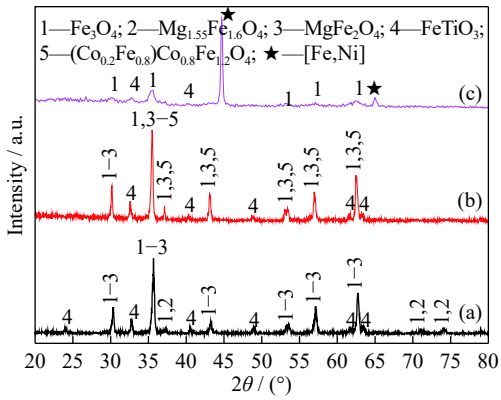

Fig. 3. XRD patterns of the NM at various stages: (a) NM; (b) after H_2 reduction at 450°C; (c) after CO_2 decomposition at 300°C.

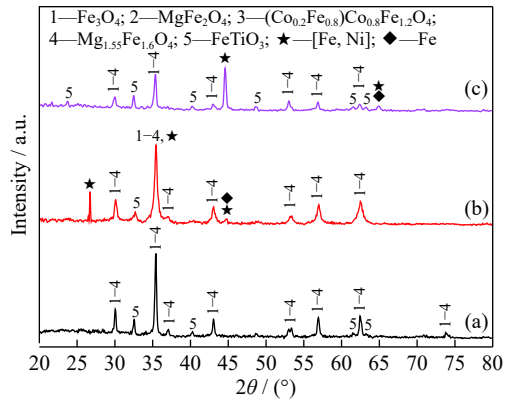

Fig. 4. XRD patterns of the MNM at various stages: (a) MNM; (b) after H_2 reduction at 450°C; (c) after CO_2 decomposition at 300°C.

after CO_2 decomposition. Based on the above results, for the MNM after H_2 reduction, its isomorphism substitutions of multi-metals effectively promote adsorption and decomposition of CO_2 due to the oxygen flooding effect formed on the surface [29]. Furthermore, the appearance of metallic phases of [Fe,Ni] and Fe indicates that there is a higher oxygen-deficient degree, which conduces to heighten the reaction selectivity of CO_2 decomposition to C. Then, the formed C could reduce the oxides of Fe or FeNi to metal phase Fe or [Fe,Ni]. These results are in good agreement with the results of the H_2-TPR and the CO_2-TPSR.

3.4. Amounts and phase forms of deposited carbon

The FE-SEM images of the samples reduced in H_2 atmosphere at 450°C for 90 min and subsequently oxidized in CO_2 atmosphere at 300°C for 90 min (*in situ*) are shown in Fig. 5. As shown in Fig. 5(a), the size distribution of the NM was very uneven and ranged from 10 to 180 μm with irregular shapes, whereas the MNM (Fig. 5(b)) took a spherical shape with an even distribution, whose particle diameter is about 0.5 μm. Although there are some larger agglomerates, their particle sizes are lower than 2.0 μm. Table 1 presents the energy-dispersive X-ray spectroscopy (EDS) results of the samples after CO_2 reduction. The increase in carbon content and decrease in oxygen content indicate that the MNM possessed a higher oxygen-deficient degree and the CO_2 reduction reaction occurs. The carbon content obtained over the MNM was 2.87wt% higher than that of NM.

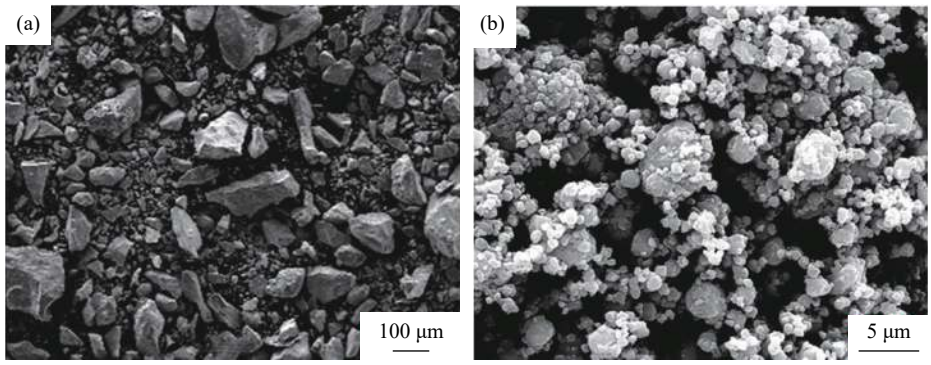

Fig. 5. FE-SEM images of the samples treated in H_2 at 450°C and CO_2 atmosphere: (a) NM; (b) MNM.

Table 1. EDS results of the samples reduced at 450°C and then oxidized at 300°C wt%

Sample	C	O	Mg	Al	Si	Ti	V	Fe
NM	3.73	30.22	2.59	2.54	0.79	7.55	0.34	52.69
MNM	6.60	25.47	1.97	2.45	2.01	7.21	0.58	54.73

To investigate the nature of carbon-containing phases (graphite, amorphous carbon, or cementite), the powder samples that were reduced in H_2 atmosphere at 450°C for 90 min and subsequently oxidized in CO_2 atmosphere at 300°C for 90 min (*in situ*) were dissolved using adequate aqueous hydrochloric acid. The XRD analysis was conducted on the undissolved substance [17−18]. No phase containing carbon was discovered, as shown in Fig. 6. Detecting the deposited carbon by XRD is difficult; thus, the Raman spectra and IR spectra were employed to further investigate the phase form

of the deposited carbon [9–12]. Fig. 7 shows the Raman spectrum profiles of the NM and the MNM after treatment in H_2 and CO_2 atmosphere. Two characteristic peaks were observed for both specimens, which is well consistent with the fact that amorphous carbon shows two broad peaks, between 1340 and 1600 cm^{-1}. The mode at about 1600 cm^{-1}, often referred to as the G mode, is assigned to the "in-plane" displacement of the carbons strongly coupled in the hexagonal sheets, while the mode at around 1340 cm^{-1} corresponds to the D mode induced disorder carbon [9–12,35–36]. Compared with the MNM, the bandwidths of both D and G modes for the NM are greater, and the intensity rates of D band to G band (I_D/I_G) are higher, indicating that deposited carbons over the NM possessed a higher defect density or a smaller crystal granule size [35−36]. As shown in Fig. 8, the species containing carbon was further confirmed by bands at about 985, 1070, and 1625 cm^{-1} in the IR profiles, which are attributed to the in-plane bending vibration of C−H, the asymmetric stretching mode of C–O–C, and the flexing oscillation of conjugated C=C, respectively [37−38]. The formation of C–H and C−O−C suggests that the deposited carbon and the magnetite substrate interacted. Accordingly, it is believed that deposited carbon is only in the amorphous form, neither graphite nor cementite form. This is significantly different from the products when unitary, binary, or ternary ferrite serves as catalyst for CO_2 reduction reaction [8–14,17–21,24,30–31]. This gives the important meaning for the ferrite recycle because the formation of graphite or cementite will lead to deactivation of the ferrite for CO_2 decomposition [11−12,23,39]. For the MNM, its high selectivity of CO_2 reduction reaction can be principally ascribed to its isomorphism substitutions of Fe, Ti, V, Co, Ni, and Al, and the high activity of MNM, ascribed to higher oxygen-deficient degree, smaller granule size, and a more stable spinel structure [9–12,19–22,24–25].

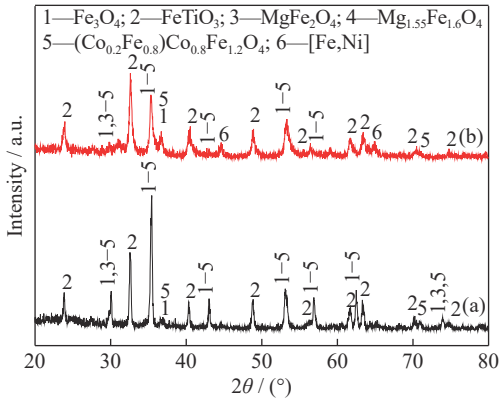

Fig. 6. XRD patterns of the undissolved substance after HCl wash for the samples, then treatment in H_2 at 450°C and CO_2 atmosphere at 300°C: (a) NM; (b) MNM.

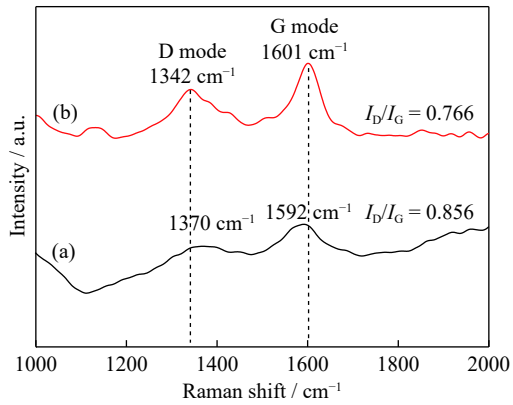

Fig. 7. Raman spectra for the samples after treatment in H_2 at 450°C and CO_2 atmosphere at 300°C: (a) NM; (b) MNM.

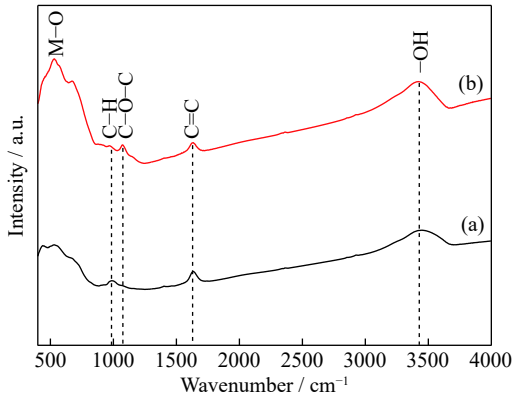

Fig. 8. IR spectra for the samples after treatment in H_2 at 450°C and CO_2 atmosphere at 300°C: (a) NM; (b) MNM.

4. Conclusion

Natural magnetite formed by isomorphism substitutions of Fe, Ti, V, Co, Ni, and Al was used as raw materials and was activated by mechanical milling and then reduced in H_2 atmosphere. Afterward, H_2-TPR and CO_2-TPSR were carried out to investigate the oxygen loss and CO_2 decomposition processes. The evolvement of the crystalline structure was investigated from mechanical milling to H_2 reduction and then to CO_2 decomposition processes. Both the NM and the MNM exhibited high selectivity of decomposing CO_2 to amorphous C. The amount of carbon deposited over the mechanically milled natural magnetite freshly reduced in H_2 gas was 2.87wt% higher than that deposited over the natural magnetite. Moreover, the high selectivity and enhanced activity of the MNM should be due to the isomorphism substitutions of Fe, Ti, V, Co, Ni, and Al; smaller granule size; higher oxygen-deficient degree; and a more stable spinel structure. Herein, a facile and "green" path is easily available for the catalyst to selectively decompose CO_2 to amorphous C.

Acknowledgements

This work was supported by the National Key Research and Development Program of China (No. 2016YFB 0600904). The authors gratefully acknowledge the support of the Analytical and Test Center of Sichuan University.

References

[1] A.Q. Chen and B.L. Lin, A simple framework for quantifying electrochemical CO_2 fixation, *Joule*, 2(2018), No. 4, p. 594.

[2] A.S. Agarwal, Y.M. Zhai, D. Hill, and N. Sridhar, The electrochemical reduction of carbon dioxide to formate/formic acid: engineering and economic feasibility, *ChemSusChem*, 4(2011), No. 9, p. 1301.

[3] D. Gao, R.M. Arán-Ais, H.S. Jeon, and B. Roldan Cuenya, Rational catalyst and electrolyte design for CO_2 electroreduction towards multicarbon products, *Nat. Catal.*, 2(2019), No. 3, p. 198.

[4] X. Tan, H.A. Tahini, H. Arandiyan, and S.C. Smith, Electrocatalytic reduction of carbon dioxide to methane on single transition metal atoms supported on a defective boron nitride monolayer: First principle study, *Adv. Theory Simul.*, 2(2019), No. 3, p. 1800094.

[5] P. Chen, B. Cui, Y.M. Bu, Z.F. Yang, and Y.Y. Wang, Synthesis and characterization of mesoporous and hollow-mesoporous $M_xFe_{3-x}O_4$ (M = Mg, Mn, Fe, Co, Ni, Cu, Zn) microspheres for microwave-triggered controllable drug delivery, *J. Nanopart. Res.*, 19(2017), No. 12, p. 398.

[6] H.P. He, Y.H. Zhong, X.L. Liang, W. Tan, J.X. Zhu, and C.Y. Wang, Natural Magnetite: An efficient catalyst for the degradation of organic contaminant, *Sci. Rep.*, 5(2015), No. 1, p. 10139.

[7] M. Munoz, Z.M. de Pedro, J.A. Casas, and J.J. Rodriguez, Preparation of magnetite-based catalysts and their application in heterogeneous Fenton oxidation – A review, *Appl. Catal. B*, 176-177(2015), p. 249.

[8] M.S. Fu, L.S. Chen, and S.Y. Chen, Preparation, structure of doped ferrite and its performance of decomposition of carbon dioxide to carbon, *Chem. J. Chin. Univ.*, 26(2005), No. 12, p. 2279.

[9] L.J. Ma, L.S. Chen, and S.Y. Chen, Study of the CO_2 decomposition over doped Ni-ferrites, *J. Phys. Chem. Solids*, 68(2007), No. 7, p. 1330.

[10] L.J. Ma, L.S. Chen, and S.Y. Chen, Study on the cycle decomposition of CO_2 over $NiCr_{0.08}Fe_{1.92}O_4$ and the microstructure of products, *Mater. Chem. Phys.*, 105(2007), No. 1, p. 122.

[11] L.J. Ma, L.S. Chen, and S.Y. Chen, Studies on redox H_2−CO_2 cycle on $CoCr_xFe_{2-x}O_4$, *Solid State Sci.*, 11(2009), No. 1, p. 176.

[12] L.J. Ma, L.S. Chen, and S.Y. Chen, Study on the characteristics and activity of Ni−Cu−Zn ferrite for decomposition of CO_2, *Mater. Chem. Phys.*, 114(2009), No. 2-3, p. 692.

[13] Y. Tamaura and M. Tahata, Complete Reduction of carbon-dioxide to carbon using cation-excess magnetite, *Nature*, 346(1990), No. 6281, p. 255.

[14] C.L. Zhang, T.H. Wu, H.M. Yang, Y.Z. Jiang, and S.Y. Peng, Reduction of carbon-dioxide to carbon with active cation excess magnetite, *Chem. J. Chin. Univ.*, 16(1995), No. 6, p. 955.

[15] H.M. Yang, C.L. Zhang, T.H. Wu, Y.Z. Jiang, and S.Y. Peng, Preparation of $Fe_{3+\delta}O_4$ and their complete decomposition of CO_2 to carbon, *Acta. Chim. Sinica*, 53(1995), No. 11, p. 1101.

[16] S. Álvarez-Torrellas, M. Munoz, V. Mondejar, Z.M. de Pedro, and J.A. Casas, Boosting the catalytic activity of natural magnetite for wet peroxide oxidation, *Environ. Sci. Pollut. Res.*, 27(2020), No. 2, p. 1176.

[17] E. Yamasue, H. Yamaguchi, H. Nakaoku, H. Okumura, and K.N. Ishihara, Carbon dioxide reduction into carbon by mechanically milled wustite, *J. Mater. Sci.*, 42(2007), No. 13, p. 5196.

[18] E. Yamasue, H. Yamaguchi, H. Okumura, and K.N. Ishihara, Decomposition of carbon dioxide using mechanically-milled magnetite, *J. Alloys Compd.*, 434(2007), p. 803.

[19] J.S. Kim and J.R. Ahn, Characterization of wet processed (Ni, Zn)-ferrites for CO_2 decomposition, *J. Mater. Sci.*, 36(2001), No. 19, p. 4813.

[20] J.S. Kim, J.R. Ahn, C.W. Lee, Y. Murakami, and D. Shindo, Morphological properties of ultra-fine (Ni,Zn)-ferrites and their ability to decompose CO_2, *J. Mater. Chem.*, 11(2001), No. 12, p. 3373.

[21] C. Nordhei, K. Mathisen, I. Bezverkhyy, and D. Nicholson, Decomposition of carbon dioxide over the putative cubic spinel nanophase cobalt, nickel, and zinc ferrites, *J. Phys. Chem. C*, 112(2008), No. 16, p. 6531.

[22] C. Nordhei, K. Mathisen, O. Safonova, W. van Beek, and D.G. Nicholson, Decomposition of carbon dioxide at 500°C over reduced iron, cobalt, nickel, and zinc ferrites: A combined XANES−XRD study, *J. Phys. Chem. C*, 113(2009), No. 45, p. 19568.

[23] L.S. Chen, S.Y. Chen, and G.L. Lu, Study the structure stability of $NiFe_{2-x}Cr_xO_4$ (x=0, 0.08) during H_2/CO_2 cycle reaction, *J. Mater. Sci.*, 41(2006), No. 19, p. 6465.

[24] M.H. Khedr and A.A. Farghali, Microstructure, kinetics and mechanisms of CO_2 catalytic decomposition over freshly reduced nano-crystallite $CuFe_2O_4$ at 400−600°C, *Appl. Catal. B*, 61(2005), No. 3-4, p. 219.

[25] M.H. Khedr, A.A. Omar, and S.A. Abdel-Moaty, Reduction of carbon dioxide into carbon by freshly reduced $CoFe_2O_4$ nanoparticles, *Mater. Sci. Eng. A*, 432(2006), No. 1-2, p. 26.

[26] T. Kodama, Y. Kitayama, M. Tsuji, and Y. Tamaura, Methanation of CO_2 using ultrafine $Ni_xFe_{3-x}O_4$, *Energy*, 22(1997), No. 2-3, p. 183.

[27] D.G. Streets, K.J. Jiang, X.L. Hu, J.E. Sinton, X.Q. Zhang, D.Y. Xu, M.Z. Jacobson, and J. E. Hansen, Climate change - Recent reductions in China's greenhouse gas emissions, *Science*, 294(2001), No. 5548, p. 1835.

[28] J. Tollefson, Panel negotiates climate 'synthesis report', *Nature*, 450(2007), No. 7168, p. 327.

[29] M. Tsuji, T. Yamamoto, Y. Tamaura, T. Kodama, and Y. Kitayama, Catalytic acceleration for CO_2 decomposition into carbon by Rh, Pt or Ce impregnation onto Ni(II)-bearing ferrite, *Appl. Catal. A*, 142(1996), No. 1, p. 31.

[30] H.C. Shin, S.C. Choi, K.D. Jung, and S.H. Han, Mechanism of M ferrites (M = Cu and Ni) in the CO_2 decomposition reaction, *Chem. Mater.*, 13(2001), No. 4, p. 1238.

[31] C.L. Zhang, S. Li, T.H. Wu, and S.Y. Peng, Reduction of carbon dioxide into carbon by the active wustite and the mechanism of the reaction, *Mater. Chem. Phys.*, 58(1999), No. 2, p. 139.

[32] C.L. Zhang, S. Li, L.J. Wang, T.H. Wu, and S.Y. Peng, Studies on the decomposition of carbon dioxide into carbon with oxygen-deficient magnetite I. Preparation, characterization of magnetite, and its activity of decomposing carbon dioxide, *Mater. Chem. Phys.*, 62(2000), No. 1, p. 44.

[33] C.L. Zhang, S. Li, L.J. Wang, T.H. Wu, and S.Y. Peng, Studies on the decomposing carbon dioxide into carbon with oxygen-deficient magnetite II. The effects of properties of magnetite on activity of decomposition CO_2 and mechanism of the reaction, *Mater. Chem. Phys.*, 62(2000), No. 1, p. 52.

[34] H.C. Shin, J.H. Oh, J.C. Lee, S.H. Han, and S.C. Choi, The carbon dioxide decomposition reaction with $(Ni_xCu_{1-x})Fe_2O_4$ solid solution, *Phys. Status Solidi A*, 189(2002), No. 3, p. 741.

[35] C.R. Lin, C.H. Su, C.Y. Chang, C.H. Hung, and Y.F. Huang, Synthesis of nanosized flake carbons by RF-chemical vapor method, *Surf. Coat. Technol.*, 200(2006), No. 10, p. 3190.

[36] I.D. Rosca, F. Watari, M. Uo, and T. Akaska, Oxidation of multiwalled carbon nanotubes by nitric acid, *Carbon*, 43(2005), No. 15, p. 3124.

[37] M. Keiluweit, P.S. Nico, M.G. Johnson, and M. Kleber, Dynamic molecular structure of plant biomass-derived black carbon (biochar), *Environ. Sci. Technol.*, 44(2010), No. 4, p. 1247.

[38] L.S. Jia, J.J. Li, and W.P. Fang, Enhanced visible-light active C and Fe co-doped $LaCoO_3$ for reduction of carbon dioxide, *Catal. Commun.*, 11(2009), No. 2, p. 87.

[39] M. Tsuji, T. Kodama, T. Yoshida, Y. Kitayama, and Y. Tamaura, Preparation and CO_2 methanation activity of an ultrafine Ni(II) ferrite catalyst, *J. Catal.*, 164(1996), No. 2, p. 315.